

## FATIGUE ASSESSMENT OF PANARO BRIDGE: PRELIMINARY RESULTS

Francesco V. Lippi<sup>1</sup>, Walter Salvatore<sup>2</sup>

<sup>1</sup> Consorzio Pisa Ricerche  
Corso Italia, 116 - 56125 Pisa, Italy  
e-mail: f.lippi@cpr.it

<sup>2</sup> Department of Civil Engineering - University of Pisa  
Via Carlo F. Gabba, 22 - 56122 Pisa, Italy  
email: walter@ing.unipi.it

**Keywords:** Railway bridges, vibration and distortion fatigue, steel structures, experimental tests, numerical modelling, dynamic identification.

**Abstract.** *The functionality maintenance of European infrastructures like bridges is acquiring more and more importance due to the huge economic losses related to the interruption of their regular service. In particular, fatigue represents one of the most diffused failure modes occurred in steel and composite steel-concrete bridges: in fact about 80/90% of failures in steel structures are related to fracture and fatigue. Railway bridges endure million of stress cycles during their life and they are expected to be highly vulnerable to such phenomena. Moreover, phenomena like “vibration induced” and “distortion induced” fatigue are still partially uncovered by actual design codes and represent a critical aspects for the assessment of existing bridge remaining life and for the design of new bridges.*

*The European research project FADLESS “Fatigue damage control and assessment for railways bridges”, funded by the European Research Found for Coal and Steel (RFCS), aims to define innovative technical guidelines for the assessment and control of existing and new bridges with regard to fatigue phenomena induced by vibrations and distortions produced by train passage. To this purpose, the Project combines experimental and numerical techniques in order to evaluate properly the fatigue damages on critical details induced by vibration and distortion phenomena, taking into account the dynamic train-bridge interaction effects and the actual traffic spectra on European railway lines.*

*In this paper, preliminary studies performed on the Italian case study, the Panaro Bridge, are reported. In particular, results of the standard fatigue assessment according to Eurocode rules were compared with the actual fatigue damages occurred to deck secondary components to obtain a preliminary critical review of adopted fatigue assessment methodologies. Moreover, experimental tests were designed and performed on the bridge in order to identify global and local vibration modes and to evaluate the strain time-histories under train passages of critical details. Finally, experimental global/local mode shapes were compared to numerical results of the preliminary FE bridge model.*

## 1 INTRODUCTION

Fatigue is a very important failure mode for steel structures. In fact about 80/90% of failures in steel structures are related to fracture and fatigue. In particular, railway bridges endure million of stress cycles during their life and they are expected to be highly vulnerable to such phenomena. Obviously, if a bridge survive to the construction phase without any fractures occurring, fatigue will almost always precede fracture so that, in most practical cases, controlling fatigue is more important than controlling fracture. However, it is also important to design for fracture resistance because fatigue cracks eventually can grow to a critical size at which the member undergoes fracture. Several studies were performed in the past in order to assess the fatigue resistance of steel and steel-concrete composite bridges; such studies were the base of modern codes and standards [1; 2; 3; 4]. Despite of these efforts, the fatigue assessment of railway bridges both considering the design of new bridges and the assessment of existing ones is one of the main issues in current practice.

Such eventuality is due to concurrent events as for example the rapid development of the European railway networks according to the directives of the European Commission [5] the increase of passenger and freight railway traffic, the introduction of new high strength materials, the influence of particular effects like distortion and local vibration not actually covered by fatigue assessment procedures proposed by current codes and standards.

On the other hand, by 2020, new Trans-European Transport Network (TEN-T Project) will include 94 000 km of railways, including around 20 000 km of high-speed rail lines suitable for speeds of at least 200 km/h. Completing the network by 2020 involves the construction of the so-called 'missing links' which will increase the existing rail by 12 500 km. In addition, 12 300 km of rail lines will be substantially upgraded [5].

Completing the networks will have a huge impact in reducing journey time for passengers and goods. For interregional traffic alone the benefits are estimated to be almost EUR 8 billion per year. In addition, freight transport in the EU is expected to increase by more than two thirds between 2000 and 2020, and to double in the new Member States. Freight transport among Member States is expected to show the largest increase overall. Without TEN-T this increase in transport would be impossible to handle, and our rate of economic growth significantly slowed.

An important aspect in design of new lines or in the evaluation of upgrading operations is the convenience that the railway lines will not be restricted to their use by a limited family of trains. On the contrary, they should allow the transit of all vehicle typologies (both traditional, high speed and freight trains), enabling interoperability of the infrastructure by all possible trains. This issue is not only essential from a social and economical point of view, but has also other implications, such as to separate the business of the infrastructure from that of the transport operators, as suggested by the new European directive [6].

The possible presence of new train typologies, characterized by several layouts of weights and axels distributions, introduces new uncertainties on the expected traffic loads and the consequent loading spectra to be adopted in fatigue verification. As a consequence, new operating conditions of European Railway Networks require the assessment of adequacy and effectiveness of actual loading spectra provided by design codes and regulations for fatigue verification purposes. Such spectra, derived from previous studies performed on old railway lines, could lead to an underestimation of actual railway traffic effects.

The knowledge of past and current load spectra, together with predicted future loads, is essential in the evaluation and fatigue analysis of existing bridges. In particular, the information concerning actual loads is very important during rating operations according to the procedures adopted by main Railway Administrator. Therefore, there is a need for accurate and inexpen-

sive methods to determine the actual loads, the strength of the bridge, and its remaining life. There is also a need for verification of live load used for the development of a new generation of bridge design codes.

The increase of circulation speed, the change of the vehicles geometry and masses and the increase of loads that were observed led to a concern in the understanding of dynamic phenomena and in their quantification, and therefore to the improvement of safety checking procedures in structural codes. In particular, the evaluation of effective capability of existing bridges to guarantee the necessary safety level under actual traffic conditions requires the improvement of available design procedures. Figure 1 shows a general framework [7] to be adopted for the fatigue assessment of existing steel structures. Such an approach suggests the use of three different levels of assessment methodologies:

- *Simplified methods*: preliminary evaluation should be conducted by using current codes and recommendations and making conservative assumptions when information is lacking or doubtful; simplified models are adopted for the structures and their details;
- *Enhanced methods*: a detailed investigation should be performed, adopting a refined representation of the structure and of the loads/actions; anyway input data for model analysis can be adopted from current codes;
- *Advanced methods*: advanced evaluation should be carried out to analyze, by means of both numerical and experimental tools, the effective remaining fatigue life of all relevant details.

The application of different evaluation methodologies requires an increasing level of knowledge and information concerning the behaviour of structural components and details. In particular the use of advanced methodologies is actually limited to specialized laboratories and scientific research groups.

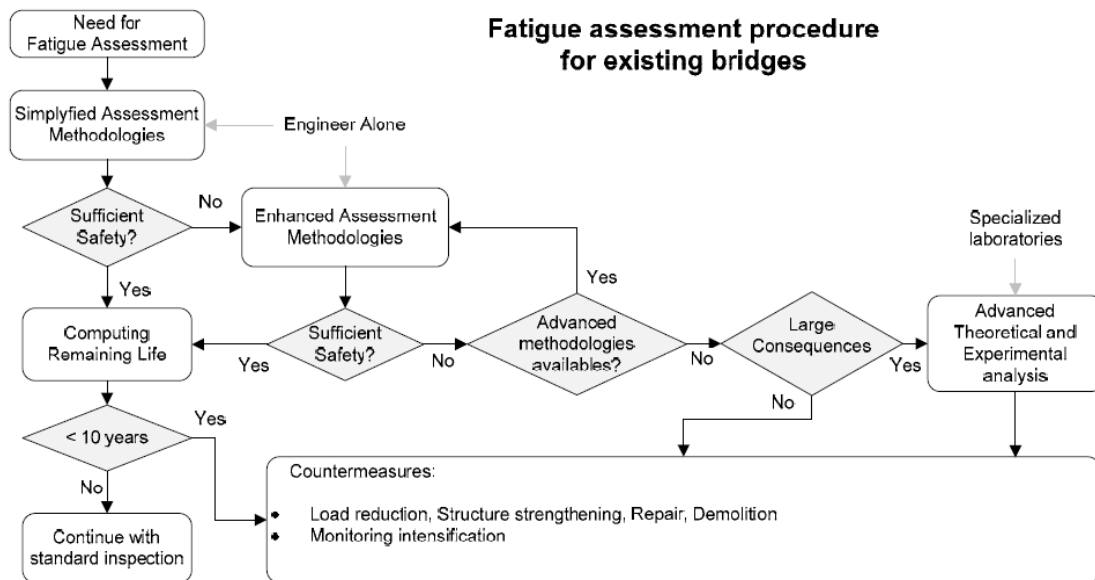


Figure 1: Fatigue assessment procedure for existing steel bridges [7].

Such an approach is mainly due to the fact that, traditionally, it was assumed that the need for the application of advanced analysis methodologies in design of steel and steel-concrete composite bridges can be limited adopting proper detailing that remove the secondary stresses. Such objectives were reached introducing an high number of global and local stiffeners, nec-

essary to guarantee the verifications of static requirements against instability as well. On the contrary, several fatigue problems affected and still affect steel bridges due to several reasons.

Previous experience shows that most cracks found in bridges were caused by distortion of member cross sections and out-of-plane deformation of webs that induced localized bending stresses [8]. In older bridges, transverse stiffeners and attachment plates were not welded to the tension flange of welded I-girders and box girders for fear that a fatigue crack initiating in the flange would lead to a brittle fracture. This well-intended but outdated practice originated in Europe in the 1930's from unexpected brittle fracture in the oldest welded bridges, and it was at first attributed to welding details, but it was primarily due to the poor quality of steel.

This practice has been the main cause of distortion-induced cracking, which can sometime be prevented by welding stiffeners to the web and to the flanges. Figure 2 shows a crack which formed along the fillet weld attaching a diaphragm connection plate to the web of a plate girder [9]. The fatigue cracking in these gaps typically occurs in a longitudinal direction along the fillet weld toe of the longitudinal web-to-flange joint, at the termination of the vertical fillet weld, or at both locations, as shown in Figure 3 [9].

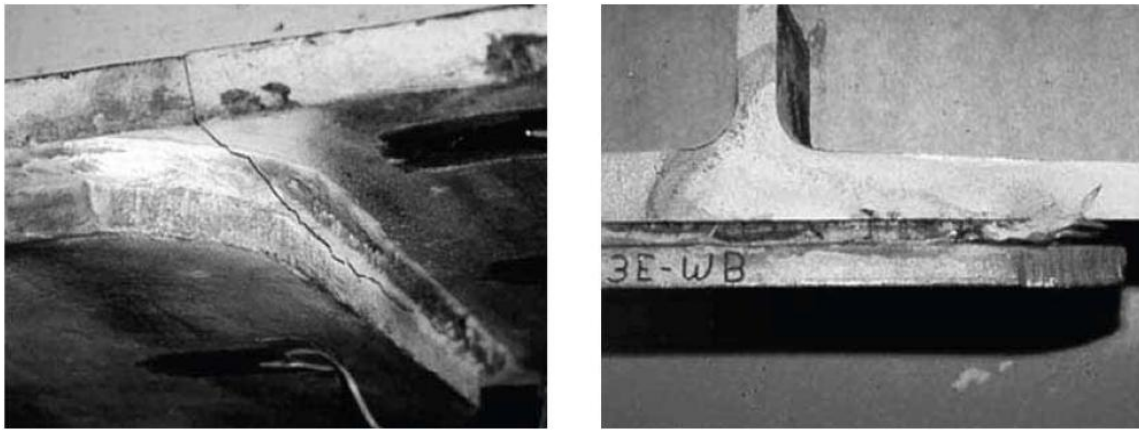


Figure 2: Examples of distortion induced fatigue crack progression [9].

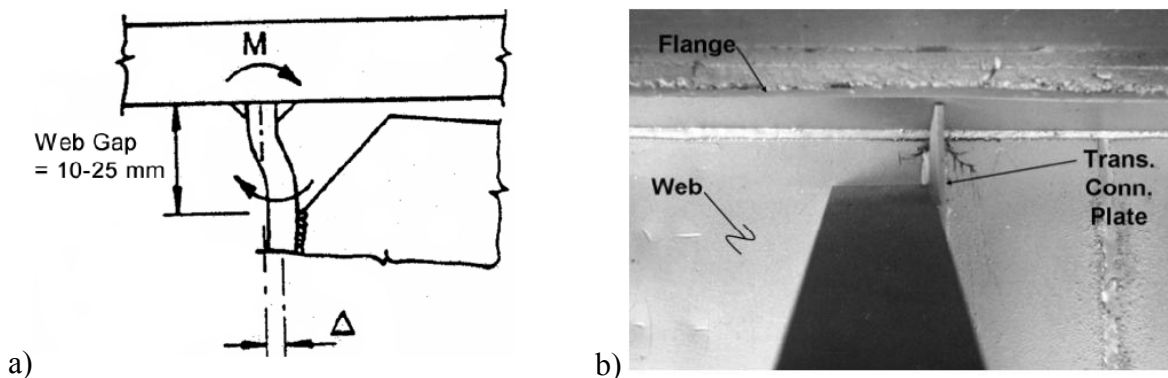


Figure 3: Web gap distortion: a) scheme of the effects; b) example in real bridge [9].

In many cases, the displacement causing this distortion is limited and the cracking arrests as the compliance of the gap increases and the stresses are reduced. Because most of the cracks are longitudinally oriented, there is typically no reason to be concerned about fracture of the girder unless the cracks turn downward and propagate across the web. It is typically a mistake to try to weld repair such cracks, as this restores the high stresses which originally caused the cracking and will certainly restart the cracking at the weld repair [9].

Besides, distortion and vibration induced fatigue phenomena, typically due to low local stiffness distribution in correspondence of critical details, can affect steel and composite bridges. Such phenomenon allows the presence of local vibration modes characterized by low frequencies (0-30 Hz) typically excited during train passages which could produce high local “modal” stresses causing relevant fatigue damages and reducing the remaining fatigue life.

As previously stated, distortion induced or vibration induced fatigue cracking in the web gaps may be solved by a proper detailing which eliminates the secondary stresses causing these cracks. In most cases, the web-gap-cracking can be prevented by rigidly connecting the attachment plates to the tension flange. Where the distortion is displacement controlled, the stresses can be reduced by increasing the flexibility of the connection. If distortion is limited, holes may be drilled or cored at the crack tips to temporarily arrest propagation [9].

Modern design methodologies for steel and steel-concrete composite bridges adopt new materials with very high performances allowing for very slender structures. Such solutions, characterized by improved performance against static loadings, revealed to be exposed to vehicle-bridge interaction effects which influence fatigue behavior.

High structural slenderness implies that non-structural elements, such as ballast, retaining walls and tracks, can affect bridges dynamic behavior caused by train passage. Moreover, the high local slenderness caused by the reduction of plate thickness and stiffeners number, can increase the possibility of obtaining local vibration modes characterized by low frequencies. As a consequence, such local modes can increase the possibility of observing “vibration induced” fatigue damage phenomena. By the way, actual codes and regulations appear inadequate to provide effective tools in order to obtain thorough information about such phenomena.

Moreover, the use of High Performance Steel does not modify the results of fatigue verifications since fatigue behavior does not depend on mechanical or dynamical properties of materials.

Local vibration and distortion phenomena do not affect only steel details/elements. In fact, both in steel-concrete connection systems (such as studs) and concrete slabs between the main girders in steel-concrete composite solutions result highly affected by such phenomena as well. In particular, it will be useful to evaluate the effective load spectra affecting reinforcement bars in concrete slabs directly subjected to the load induced by train passage and the consequent free vibrations.

Main object of the European research project FADLESS "*Fatigue damage control and assessment for railways bridges*", funded by the European Research Found for Coal and Steel (RFCS) and in course of realization, is to investigate the aforementioned uncertainties on the structural behaviour and integrity of steel and composite steel-concrete bridges with particular attention to the fatigue phenomena. To this aim, a modern procedure for the evaluation of the actual fatigue load and resistance of principal elements and critical details will be assessed for selected case studies representative of the bridge typologies most exposed to such damages.

In particular, the actual fatigue loading spectra will be evaluated taking into account the real and the expected traffic flows, also because of possible reclassification of railway lines, of the global dynamic train-bridge interaction effects and of the local dynamic vibration and distortional effects. Moreover, actual fatigue resistance of the main elements / critical details subjected to distortion induced effects will be evaluated. In such a way, it will also be possible to setup suitable strategies for the evaluation of vibration induced and distortion induced fatigue damaging in steel and composite steel-concrete railway bridges, as well for the control of the crack growth.

In this paper some preliminary results obtained for the Panaro bridge, a study case of FADLESS Project, are illustrated. In particular, standard modelling and fatigue assessment,

experimental tests, model updating and advanced fatigue assessment of Panaro bridge will be described. Objectives of such activities were to: i) investigate the actual dynamic behaviour of the structure; ii) compare the fatigue assessment results obtained by standard and advanced approaches; iii) define preliminary observations to the fatigue assessment methodologies currently adopted in European design codes. Moreover, this first part of the Project will constitute the base for future developments of the research, leading to better comprehension of vibration and distortion fatigue phenomena induced by real traffic on steel and steel-composite railway bridges.

## 2 THE PANARO BRIDGE

The bow-string steel bridge on the Panaro river, along Bologna-Verona railway line, is the very first Italian railway bridge constructed adopting welded components (Figure 4). This particular bridge, supporting two tracks, has experienced an intense passenger and freight traffic since its construction in the 70's.

The bridge has a span length equal to 75.6 meters and its cross section height varies from 7 to 11 meters (Figure 5). All main components such as lower and upper strings, vertical and diagonal beams, main cross girders, lower and upper bracing diagonals at deck ends are built-up welded members (Figures 6 and 7). All joints are constituted by riveted solutions, thus realizing a very particular structure among steel railway bridges, an uncommon mix between welded components and riveted joints. Lower and upper main bracings are present, together with secondary longitudinal beams, directly supporting the rails, and local track bracings (Figures 8 and 9). End supports are constituted by steel bearings directly in contact with lower main strings (Figures 10 and 11).



Figure 4: Picture of Panaro bridge (Courtesy of RFI).

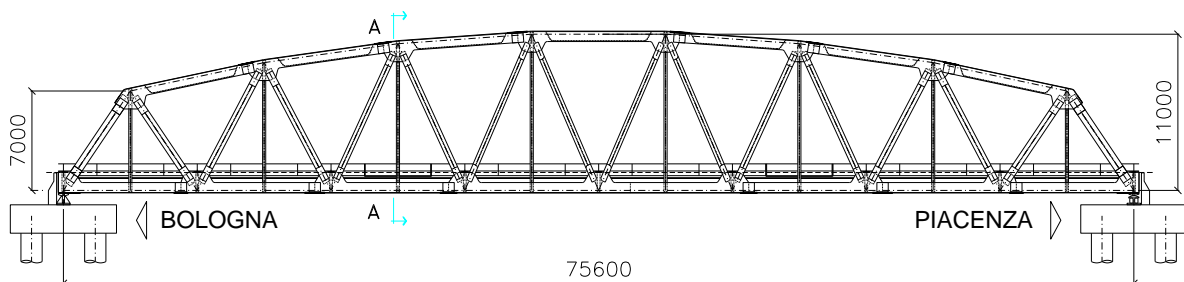


Figure 5: Drafting of Panaro bridge (Courtesy of RFI).





Figure 6: General view of Panaro bridge



Figure 7: Riveted diagonal-lower string joint of Panaro bridge



Figure 8: General view of deck structure



Figure 9: General view of lower and track bracings



Figure 10: General view of unidirectional bearing



Figure 11: General view of fixed bearing

During its exercise life, some of the secondary elements of the structures showed fatigue damages induced by distortion and vibration phenomena, as reported in Figures 12 and 13. In particular, almost all cross beams of track local bracings (originally fully fixed to the secondary longitudinal girders) experienced the same fatigue damage at the end restraints. Italian authority decided to cut the profiles in order to stop the crack propagation and changed beam end connections into pin joints removing the external bolts, in order to reduce the bending forces induced by distortion phenomena (Figure 12). Moreover, the connection between sleepers and longitudinal girders, obtained by catch bolts anchored to steel plates welded to the upper girder flanges, experienced fatigue damages in the longitudinal plate-flange welding due to vibration effects (Figure 13).



Figure 12: Typical fatigue damage and repair of track bracing cross beams



Figure 13: Sleepers-longitudinal girder connection by catch bolts

### 3 STANDARD MODELLING AND FATIGUE ASSESSMENT

Two FE beam models were developed by ANSYS® software for the standard fatigue assessment of Panaro bridge. The first model represented the bridge original resistant scheme, with track bracing cross beams fully fixed to the longitudinal girders (Full Fixed FE Model). The second model represented the actual situation as a results of the local repair interventions, with track bracing cross beams connected by hinge joints to the longitudinal girders (Hinge FE Model) (Figures 14 and 15).

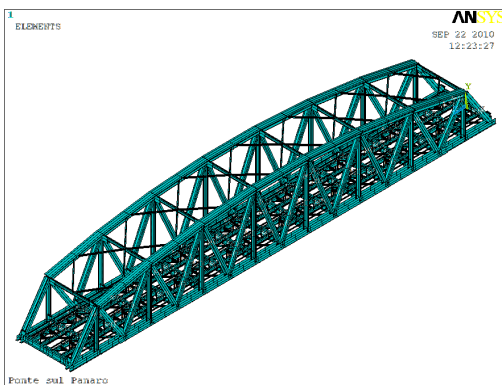


Figure 14: FEM model of the Panaro bridge

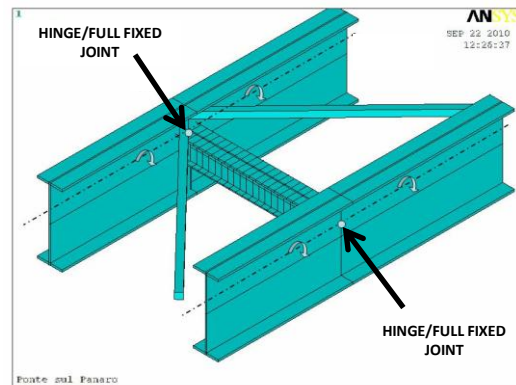


Figure 15: Track bracing cross beam connection to secondary longitudinal girders by full fixed/pin joints



All girders were represented by beam elements (BEAM188), except bracing diagonals represented by truss elements (LINK8). All elements were defined according to their actual geometrical axis and connected, where necessary, by proper internal constraints [10]. Those components characterized by variable end cross sections, as longitudinal girders, track and upper bracing cross beams, were represented by I section element in central parts and T sections elements at the ends. This approach was necessary to model properly the bridge stiffness and to obtain reliable force/stress values, as end stiffness greatly influence the intensity of in-plane and out of plane actions induced by distortion phenomena and, consequently, the intensity of local stresses (Figures from 16 to 19).

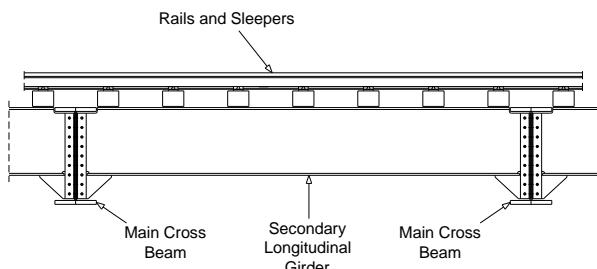


Figure 16: Side view of secondary longitudinal girders with variable end cross sections

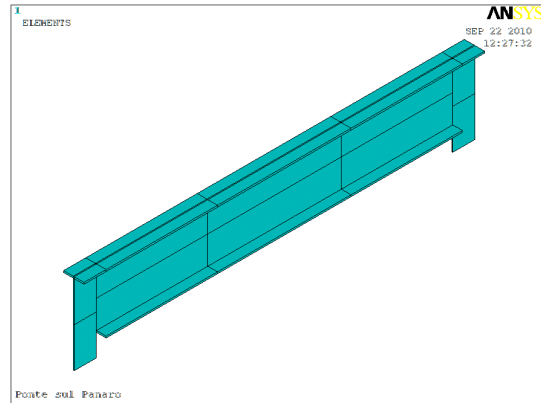


Figure 17: Local view of elements representing secondary longitudinal girders

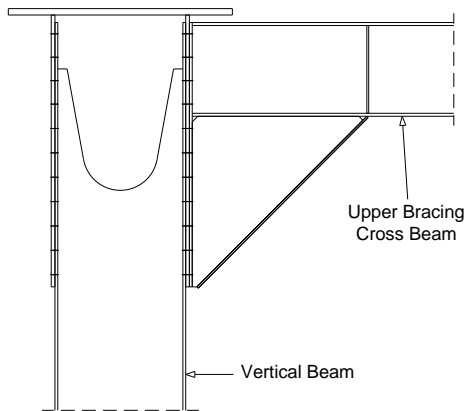


Figure 18: Side view of upper bracing cross beams with variable end cross sections

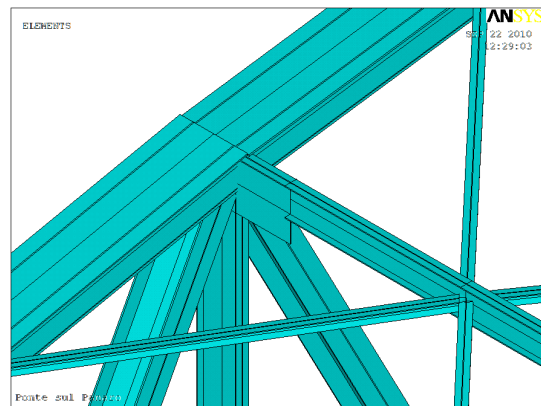


Figure 19: Local view of elements representing upper bracing cross beams

The evaluation of dynamic forces induced by train passages into the bridge components was performed according to the Eurocode rules. In particular, element stresses were calculated by incremental dynamic analysis of bridge models subjected to the moving loads of Standard and Heavy train traffic mixes [11]. The total number of train passages was calculated assuming a life cycle of 100 years.

As Eurocode fatigue train models are characterized by different lengths and velocities, the passage of each model was simulated assuming different sampling frequency in order to optimize the calculation times. In particular, analysis frequencies were calculated in such a way that the distance covered by loads between two subsequent steps was equal to 1/10 of secondary longitudinal girder length for each train velocity (Table 1).

In the dynamic analysis, damping characteristics of bridge components were represented assigning to each element a proper value of material damping, calculated as a function of length as specified by Eurocode [11]. Calculated girder material damping varied in the range 0.5% - 2.81%.

Beam element stresses were extracted from the FE models and elaborated in order to calculate the stress time-histories acting on net cross sections. In particular, the four possible combinations of normal stresses induced by the axial force and the two bending moments were considered for each element section. Moreover, vertical and transverse shear stresses acting at end restraint sections of main cross girders and upper bracing cross beams were also considered.

Normal and shear stress spectra were evaluated by rainflow counting technique. Fatigue damages were calculated independently adopting the linear damage accumulation rule of Palmgren-Miner. Fatigue classes of welded built-up members were assumed according to the indications of Eurocode [11], while for riveted components the fatigue classes proposed by Taras and Greiner were considered [12]. Fatigue classes of all bridge components are reported in Table 2.

Train Type	Vel [Km/h]	Length [m]	Analysis Frequency [Hz]
1	200	262.1	120
2	160	281.1	95
3	250	385.52	150
4	250	237.6	150
5	80	270.3	50
6	100	333.1	60
7	120	169.5	75
8	100	212.5	60
9	120	134.8	75
10	120	129.6	75
11	120	198.5	75
12	100	212.5	60

Table 1: Values of frequencies adopted in the dynamic analysis

Constructional detail	Bridge Components	Fatigue Class
One-shear joint with gusset plate	Main Lower and Upper Strings; Main Vertical Beams; Main Diagonals Beams; Main Cross Beams at end sections; Lower and Upper Bracing Diagonals	85 for normal stresses
Structural element with holes subject to bending and axial forces	Main Cross Beams at intermediate sections; Secondary Longitudinal Girders at end sections; Upper Bracing Cross Beams at intermediate Sections	90 for normal stresses
Built-up sections with automatic fillet weld	Secondary Longitudinal Girders at intermediate sections; Track cross beams at intermediate sections	125 for normal stresses
Tee-butt joints with fillet welds	Track cross beams at end sections; Upper Bracing Cross Beams at End Sections	36 for normal stresses 80 for shear stresses

Table 2: Fatigue classes adopted for Panaro bridge components

For each element section, the fatigue damage  $D_i$  induced by the  $i$  train type was calculated adopting the following simplified approach [1]:

$$D_i = D_{\sigma, \max} + D_{tv} + D_{th} \quad (1)$$

where  $D_{\sigma, \max}$  is the maximum damage induced by normal stresses considering the combinations of axial force and bending moments,  $D_{tv}$  is the vertical shear damage and  $D_{th}$  is the horizontal shear damage. Total fatigue damages obtained from Full Fixed and Hinge Model FE models for Standard and Heavy traffic mixes are reported in Figures from 20 and 24.

Considering the Full Fixed FE Model, that represents the original resistance scheme of Panaro Bridge, it is possible to observe that a significant number of elements showed a fatigue damage greater than 0.1 both for Heavy and Standard traffic mixes. Damage values between 0.1 and 1 were observed on almost all vertical beams while more severe damages, greater than 1, occurred at the end cross sections of track bracing cross beams (as really occurred) and at the connection joints of vertical beams with lower/upper stringers (actually undamaged) (Figure 22). From this point of view, more refined analysis of identified critical details seemed to be necessary for a proper evaluation of actual stress spectra.

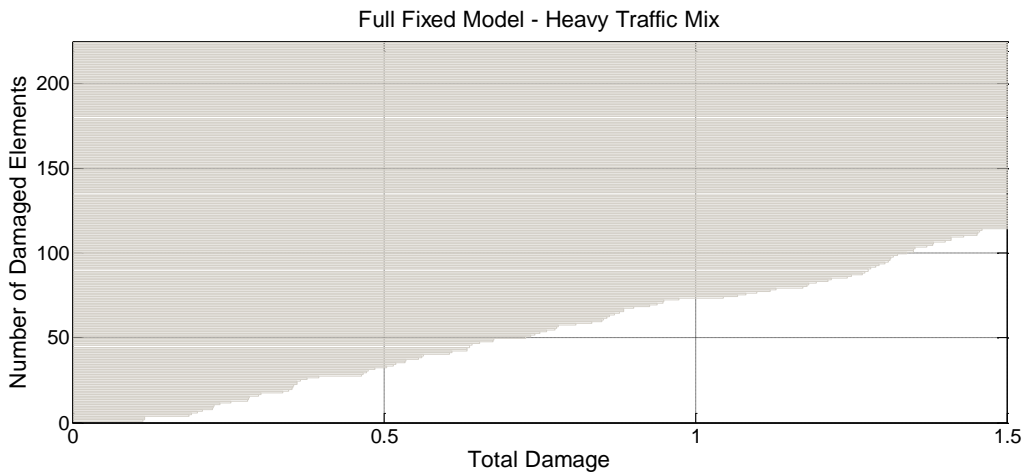


Figure 20: Full fixed FE model - Heavy Traffic Mix Damage

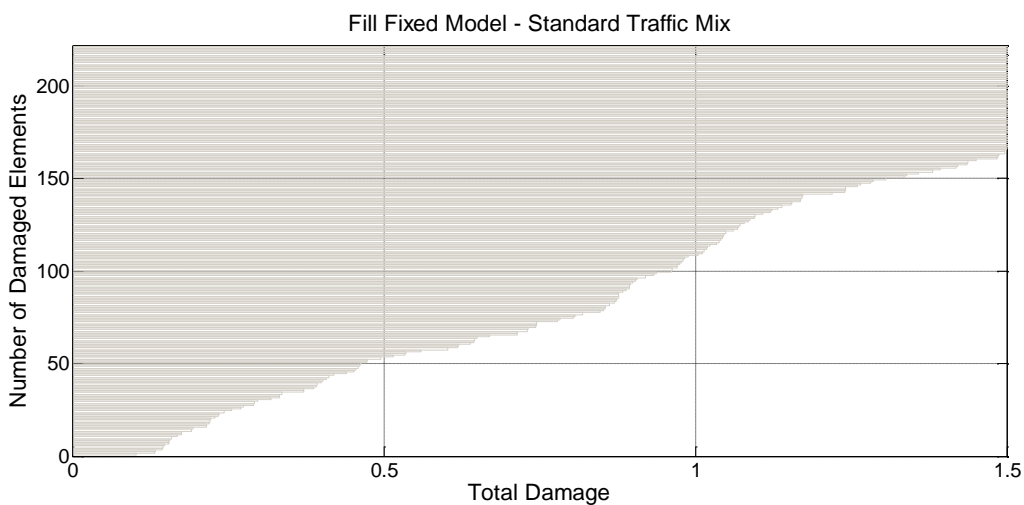


Figure 21: Full fixed FE model - Standard Traffic Mix Damage

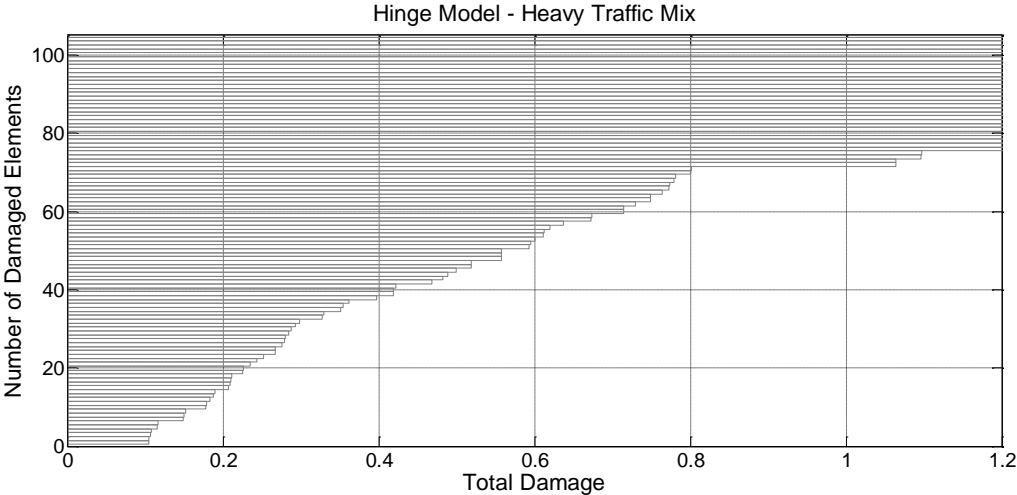


Figure 23: Hinge FE Model - Heavy Traffic Mix Damage

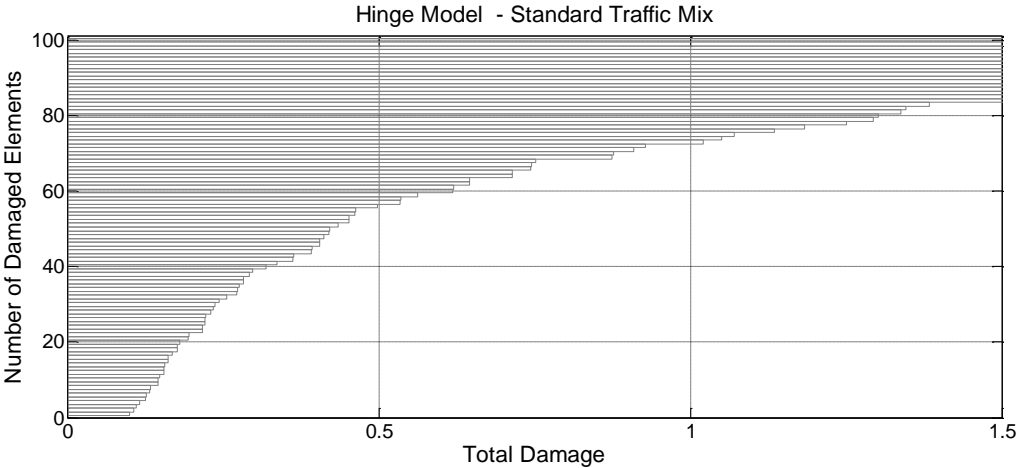


Figure 24: Hinge FE Model - Standard Traffic Mix Damage

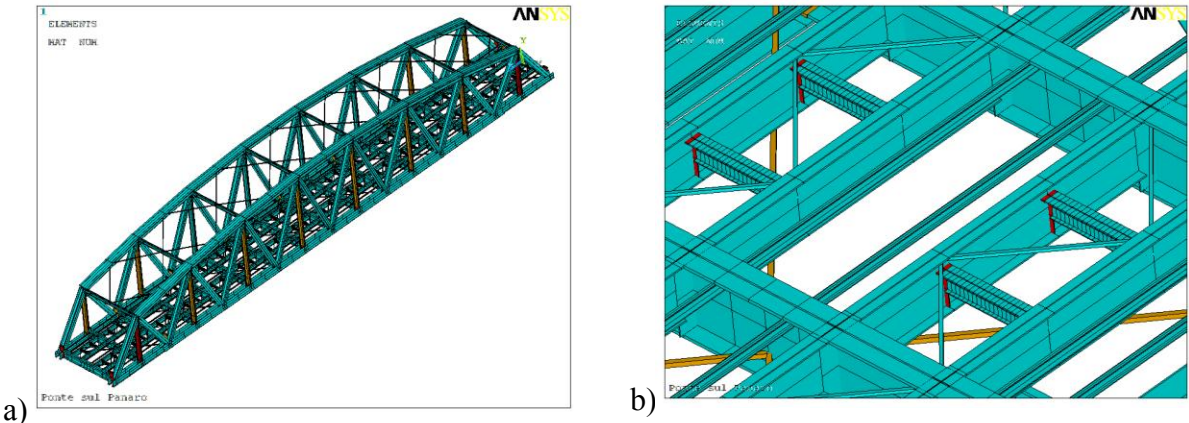


Figure 25: Full Fixed FE Models - Heavy Traffic Mix: general (a) and detailed (b) graphical representation of damaged components (Yellow elements:  $-0.1 < \text{Damage} < 1$  --- Red elements:  $\text{Damage} > 1$ )



Also for the Hinge FE Model a great number of damaged components was observed for Heavy and Standard traffic mixes. Vertical beams showed damage values between 0.1 and 1 and more severe damages, greater than 1, occurred at the connection joints of vertical beams with lower/upper stringers. Nevertheless in the Hinge Model case, that represents the actual resistant scheme of Panaro bridge, the elements representing the end sections of track bracing cross beams did not show any fatigue damage. From these results, it is possible to observe that the local modification of the track bracing cross beams practically cancelled the distortion induced local forces while did not introduce significant variations in the global structural response of the bridge.

It is important to notice in both the Full Fixed and Hinge FE Models the reliability of calculated results is unknown, as expected fatigue damages in some cases really occurred but in others didn't. So, advanced FE models of critical details are necessary in order to obtain a correct evaluation of local stresses. From this point of view, the modelling experience of Panaro bridge confirmed the necessity of advanced analysis approaches in the design of new complex structures and in the assessment of older ones, as the use of standard techniques only could lead to an erroneous evaluation of local effects.

## 4 EXPERIMENTAL TESTS

Usually steel bridges show a real structural behaviour different from the theoretical one, as every modelling and analysis technique actually available is necessary a simplified representation of more complex structures. From this point of view, experimental tests are very effective tools for the evaluation of real forces and stresses acting into bridge steel components and, consequently, can be adopted as a useful base for a reliable evaluation of fatigue performance.

The experimental tests on Panaro bridge were focused on the structure dynamic identification and on evaluation of the effects induced by train passages. In particular, global and local vibration modes were identified by operative modal analysis technique (OMA) using the ambient vibrations (white noise) as excitation source. Moreover, the effects of train passages were investigated directly recording the strain time-histories on critical details and the horizontal displacement time-histories of the deck unidirectional bearings. Such tests permitted to improve the knowledge of the real structural behaviour and constituted the base for the numerical updating of FE bridge model.

### 4.1 Global/Local Experimental Dynamic Tests

The experimental dynamic analysis on Panaro bridge was performed in order to obtain the identification of the global vibration modes and, moreover, to evaluate the dynamic characteristics of track bracing cross beams. To this aim, accelerations in the vertical, horizontal and longitudinal directions of suitable structure key points were recorded assuming the ambient vibration as excitation source.

In particular for the identification of global vibration modes, structure accelerations were recorded on eleven sections adopting a multi-step approach, that consists of acquiring data by moving sensors along the structure and keeping some of them fixed as "reference" (Figures 25, 26 and 27 ). Such "reference" sensors are adopted as common base for merging the vibration modes identified by different recording configurations, thus providing the global identification of the structure [13]. Accelerations were recorded by PCB sensors and LMS Scadas acquisition unit adopting a sampling frequency of 400 Hz for time periods of 15 minutes at least. Some train passages occurred during the acquisition of ambient sources, nevertheless such noises were afterwards cleared from recorded signals before the numerical identification of natural vibration modes, obtained by PolyMAX algorithm [13].

Seven global modes of vibration were clearly identified during the experimental tests. Modal frequencies, damping values and mode shapes are reported in Table 3, together with the mode phase collinearity values (MPC) that is equal to the unity when the complex modal displacement of all recorded nodes have the same phase (i.e. the mode is real). The modal shape extracted for the identified modes are reported in Figure 28.

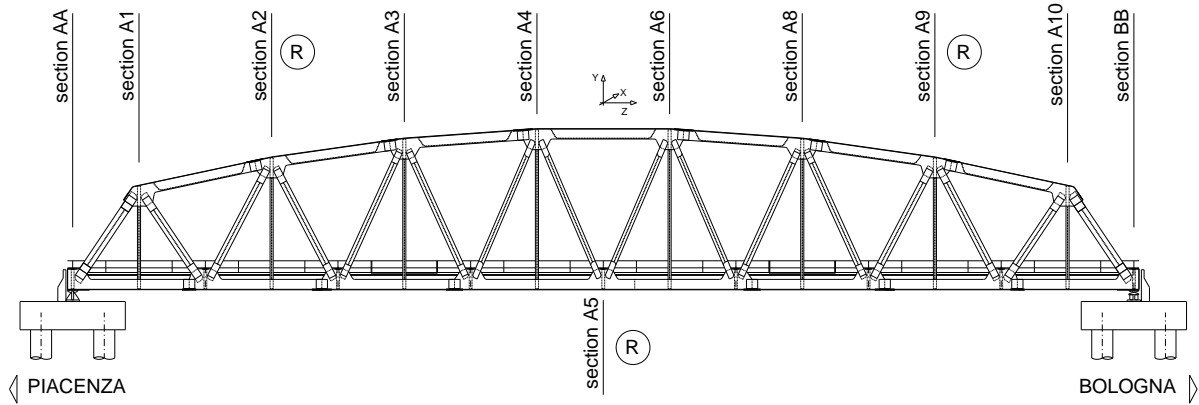


Figure 25: Global dynamic test of Panaro Bridge: test layout

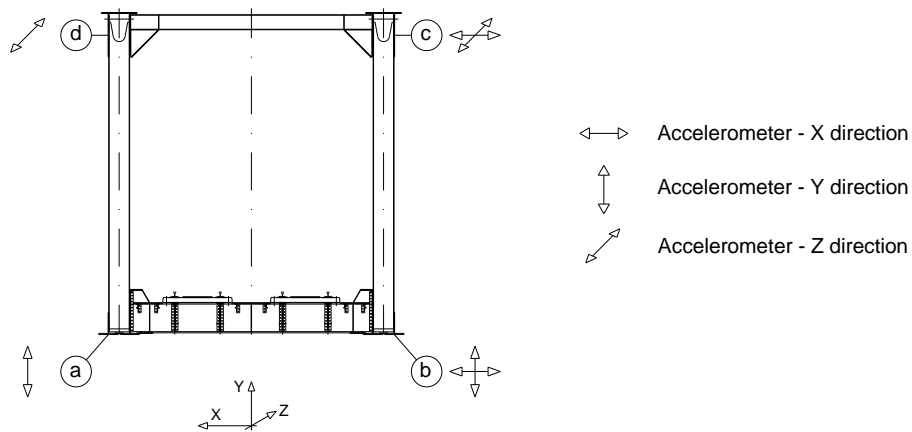


Figure 26: Global dynamic test of Panaro Bridge - position and orientation of sensors on the typical cross section

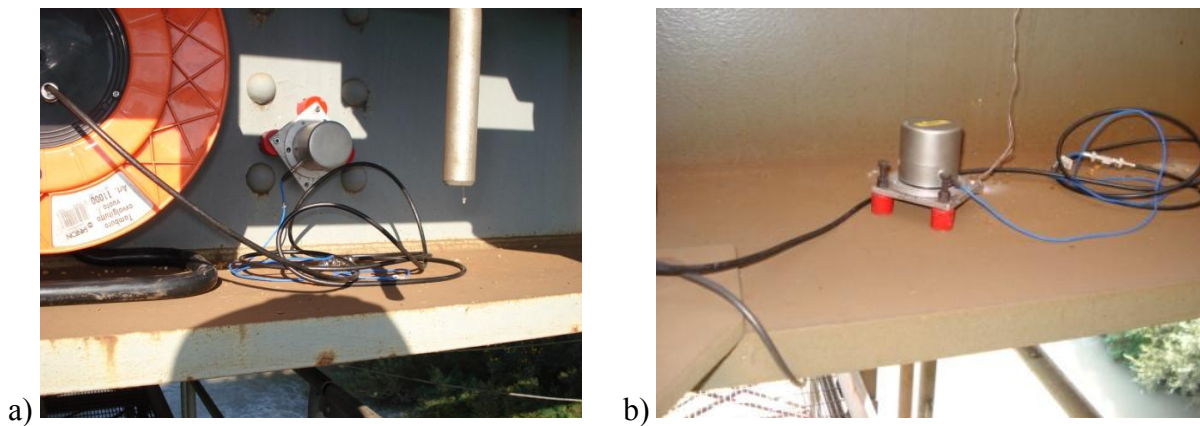


Figure 27: Horizontal (a) and vertical (b) accelerometers on main lower string

Mode n°	Frequency [Hz]	Damping [%]	MPC	Mode Shape
1	1.77	0.49		Lateral Bending
2	3.65	0.15		Torsional
3	3.68	0.65		Vertical Bending
4	4.08	0.29		Lateral Bending
5	6.86	0.15		Distortional
6	10.93	0.24		Torsional
7	12.35	0.25		Vertical Bending

Table 3: Identified global vibration mode of Panaro bridge.

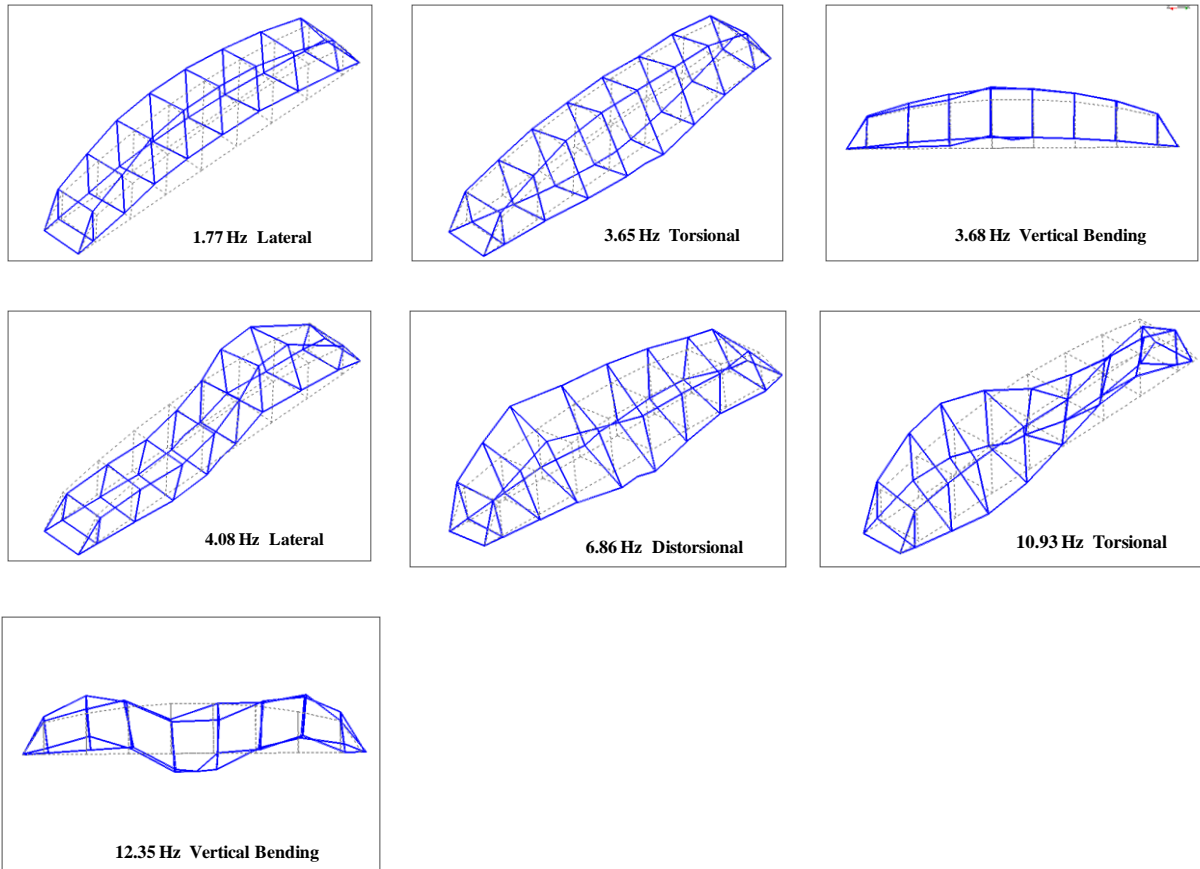


Figure 28: Panaro bridge - shapes of identified global vibration mode

Local dynamic tests were performed on a track bracing cross beam, recording vertical and transverse accelerations of upper flange at midspan and lateral sections (Figure 29). In this case, a single acquisition of all instrumented sections, realized adopting the same recording settings of global tests, permitted to identified clearly three local vibration modes of the cross beam. Modal parameters are reported in Table 4 while the calculated modal shapes are illustrated in Figure 30.

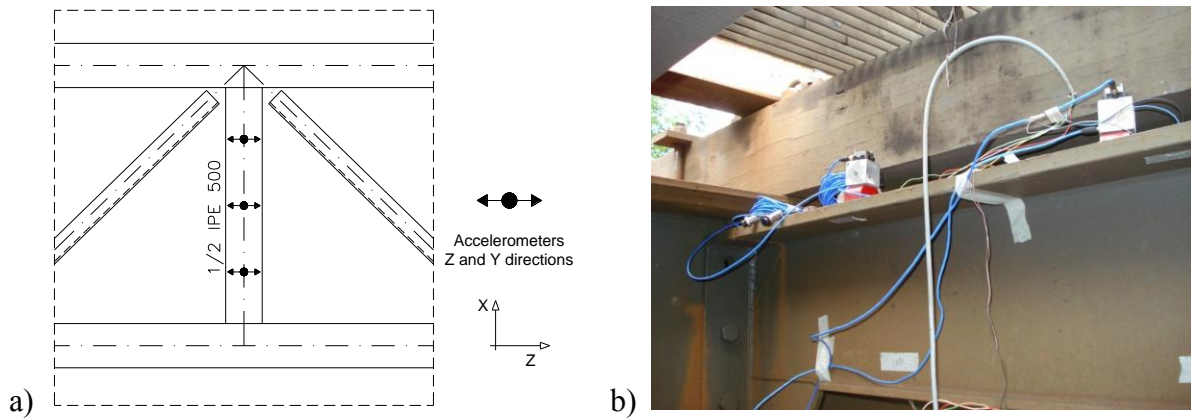


Figure 29: Instrumented sections (a) and sensors positioning (b) for the local cross beam dynamic tests.

Mode n°	Frequency [Hz]	Damping [%]	MPC	Mode Shape
1	15.65	0.82		Vertical Bending
2	44.18	0.46		Lateral Bending
3	97.22	0.56		Lateral Bending

Table 3: Identified local vibration modes of track bracing cross beam.

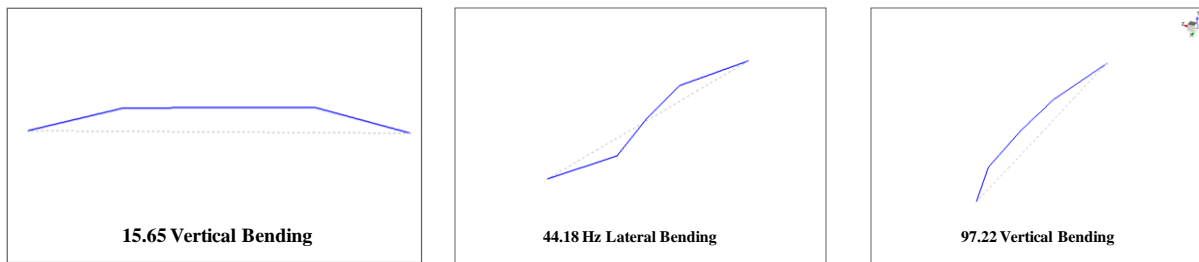


Figure 30: Panaro bridge - vibration mode shapes of track bracing cross beam

## 4.2 Strain/Displacement Experimental Tests

The effects of train passages were investigated analyzing strains of local details and displacements of external bearings.

In particular, strain time-histories were recorded on the track bracing cross beams and on the steel plates connecting sleepers to the secondary longitudinal girders (Figure 31). It was so possible to investigate the stresses actually induced into track cross beams by distortion phenomena, indirectly evaluating also the effects on internal forces of end restraint modifications from full fixed to hinge joints. Moreover, stress cycles acting into sleeper supporting steel plates were investigated as such secondary components showed extensive fatigue damages due to the vibration of track sleepers.

Stresses induced by train passages into the track bracing cross beam are very low, thus confirming that actually this component is not particularly subjected to distortion phenomena. On the contrary, more intensive actions are present into the sleeper supporting plates, due to distortion and vibration effects induced by sleeper movements under train passages. Such stresses caused extensive fatigue damages on the longitudinal welding connecting supporting



steel plates to the upper flange of secondary longitudinal girders. Stress time-histories recorded at midspan section of track bracing cross beam (CH 4) and at the sleeper supporting plate (CH 10) are reported in Figures 32 and 33.

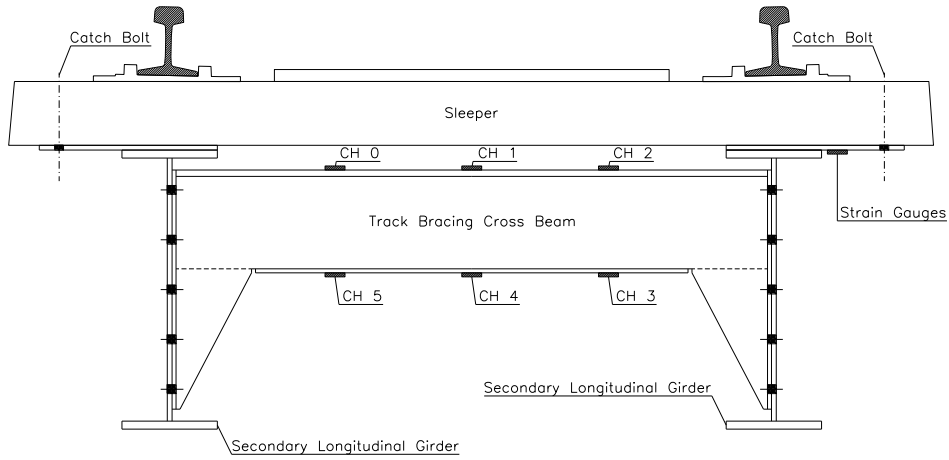


Figure 31: Strain gauge position on track bracing cross beam and sleeper supporting plates.

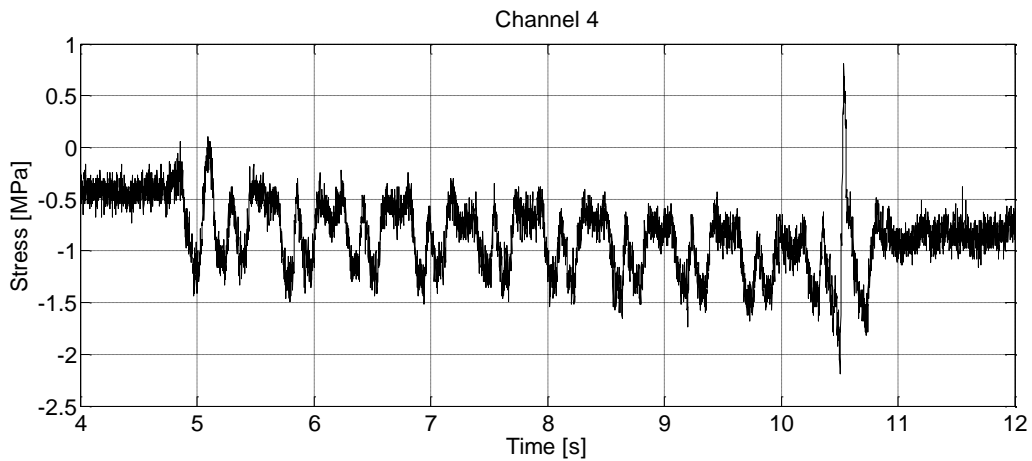


Figure 32: Midspan section of track bracing cross beam: strain time-history (CH 4)

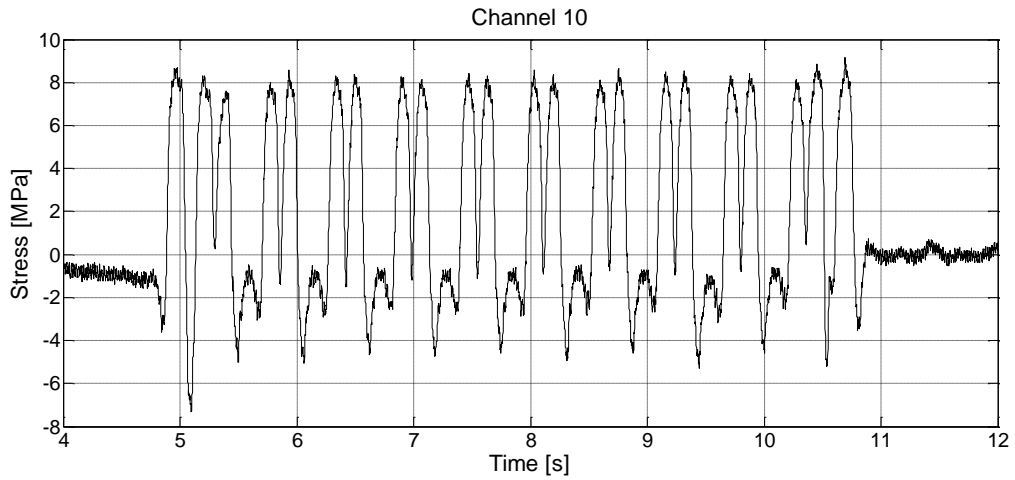


Figure 33: Strain time-history of sleeper supporting plate (CH 10)

Longitudinal movements of the two unidirectional external bearings were recorded using dynamic optoNCDT laser transducers (Figure 34). It was so possible to investigate the actual horizontal displacement time-histories of Panaro bridge under the passage of different train typologies (an example of recorded signals is reported in Figure 35). The different values of longitudinal displacements recorded for the two external bearings are probably due to torsional/lateral movements induced by asymmetric train passages on the bridge deck. The entity of such lateral bending and torsion depends on train composition, axle loads and speed. From this point of view, such results confirmed the need of considering not only vertical bending but also lateral bending and torsion in order to obtain a reliable evaluation of the dynamic structural response of such complex structures.

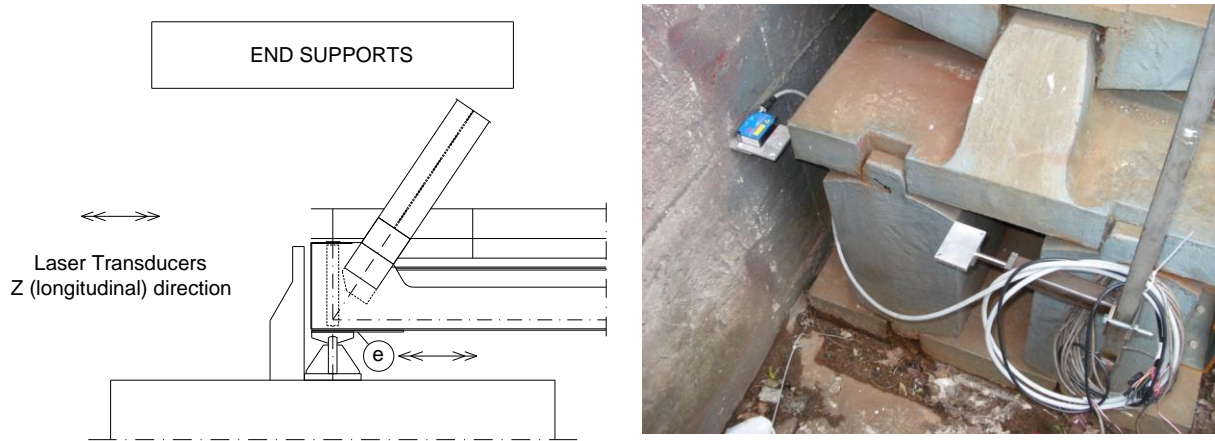


Figure 34: Laser transducers for the analysis of longitudinal bearing movements under train passages

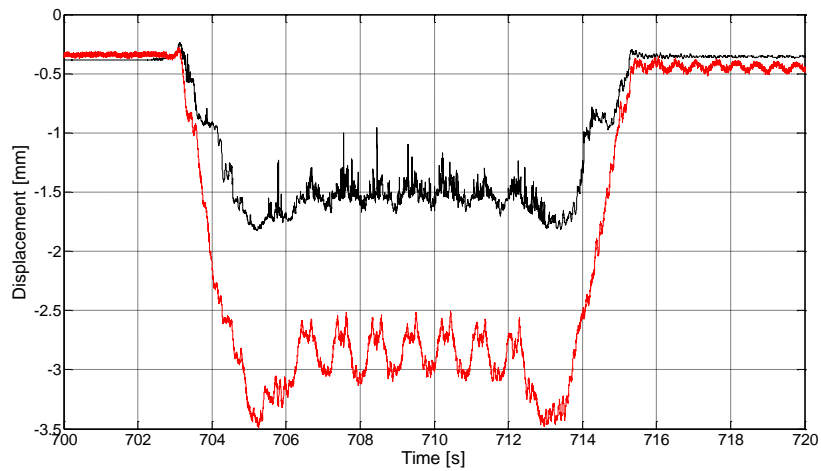


Figure 35: Example of bearing longitudinal displacements under train passages

## 5 NUMERICAL UPDATING

The global vibration modes identified in the experimental dynamic tests were adopted as reference for the numerical updating of the FE Hinge model of Panaro bridge, that represents the actual resistant scheme of the structure. To this aim, an automatic optimization procedure was implemented by MODEFRONTIER software (Figure 36). Objective of developed proce-

dure was to minimize simultaneously and independently the differences between experimental and numerical eigenfrequencies by the variation of suitable parameters.

In each sequence cycle, parameter values were changed according to the MOGA-II optimization algorithm and transferred to the ANSYS FE model, in order to extract the first twenty eigenfrequencies and vibration mode shapes [14]. Calculated results were then elaborated by MATLAB to match experimental and numerical mode of vibrations. Mode matching between  $i^{th}$  experimental and  $j^{th}$  numerical vibration modes was obtained searching the highest  $MAC_{ij}$  value, where  $MAC_{ij}$  is the modal assurance criterion calculated for  $\phi_i$  and  $\phi_j$  mode shapes normalized to the unity.

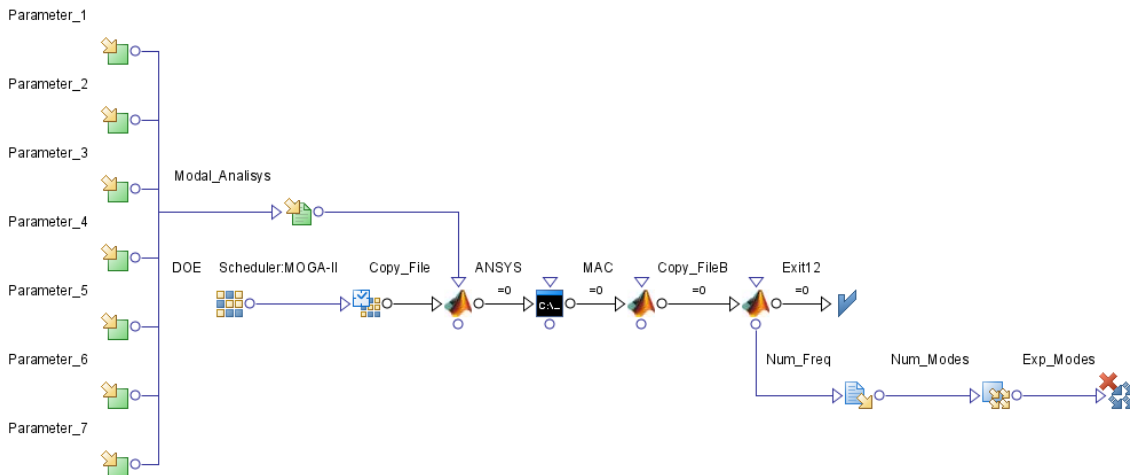


Figure 36: Optimization scheme developed for the FE model updating

After the optimization procedure was calibrated, suitable mechanical parameters had to be selected before the updating of Panaro bridge FE Hinge model. From a preliminary comparison between numerical and experimental vibration modes, a large difference between frequency values was observed, especially for those modes that involve transverse movements (lateral bending and torsion), as reported in Table 4. Some modifications were so introduced into the FE Hinge model before updating, in order to improve the numerical representation of bridge dynamic properties (Table 4).

The rotation center of end bearings, originally assumed at the contact point with the main lower stringers, was moved in the downward direction, using a mass less point element (MASS21), and its position was assumed as an optimization parameter. This modification was due to the observation that the upper bearing surfaces have a circular shape with a unknown radius, with the consequence that the rotation center is lower than the contact point.

Moreover, bearing stiffness were also represented into the FE model by spring elements (COMBIN14). In particular, longitudinal and torsional (rotation along the vertical axis) stiffness of fixed vertical bearings were modeled, while for unidirectional bearings only torsional spring elements were considered. Bearing stiffness were assumed as optimization parameters and their initial values were estimated by two FE models of fixed and unidirectional bearings subjected to unit longitudinal displacement or unit vertical rotation (Figure 37). Spring elements were directly connected to the point elements representing the rotation center of bearings. Vertical/transverse and longitudinal rotation DOFs of point elements representing the rotation center of unidirectional bearings were fixed, while for fixed bearing the longitudinal DOF was also fixed.

At least, also the values of dead loads, represented by equivalent densities of bridge components supporting secondary structures, were assumed as optimization parameters for the FE model updating. All selected optimization parameters are reported in Table 5.

Mode n°	Exp. [Hz]	Mode Shape	FE Hinge Model [Hz]	$\Delta$ [%]	Modified FE Hinge Model [Hz]	$\Delta_M$ [%]
1	1.77	Lateral Bending	2.284	29.0	1.96	10.5
2	3.65	Torsional	3.844	5.3	3.56	2.4
3	3.68	Vertical Bending	3.989	8.4	3.69	0.4
4	4.08	Lateral Bending	4.864	19.2	4.15	1.8
5	6.86	Distortional	7.377	7.5	6.65	3.0
6	10.93	Torsional	11.829	8.2	10.56	3.4
7	12.35	Vertical Bending	13.763	11.4	12.92	4.6

Table 4: Comparison between numerical and experimental modal frequencies

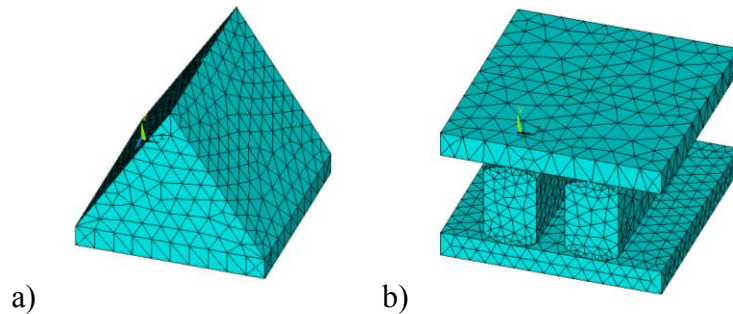


Figure 37: FE models of fixed (a) and unidirectional (b) bearings

Parameter n°	Description	Value
1	General material density of beam elements (dead weight of components, rivets and connecting plates)	9027.5 kg/m <sup>3</sup>
2	Material density of upper stringer elements (dead weight of components, rivets, connecting plates, suspended upper runaways)	17477 kg/m <sup>3</sup>
3	Material density of secondary longitudinal elements (dead weight of components, rivets, connecting plates, rails, sleepers, walking grates)	16854.6 kg/m <sup>3</sup>
4	Distance between lower stringer axis and bearing centre of rotation	0.174 m
5	Torsional stiffness of fixed bearing	124860 kN* m/rad
6	Torsional stiffness of unidirectional bearing	230690 kN* m/rad
7	Longitudinal stiffness of fixed bearing	1068800 kN/m

Table 5: Selected optimization parameters for numerical updating of Panaro FE model

The sensitivity functions of parameters n° 1-2-3 calculated for the 1<sup>st</sup>, 3<sup>rd</sup> and 4<sup>th</sup> vibration modes are reported in Figures 38a, 38b and 38c. The variation of such density parameters



have a great influence on numerical values of the eigenfrequencies, while a variation of bearing stiffness parameters (n° 5-6-7) lower than 25% did not induced significant variations.

The distance of the bearing rotation centers from lower stringer axis influenced the eigenfrequencies of modes n° 1-3-5-6-7 in the range 0-20 m, while for greater values the frequencies of aforesaid vibration modes could be considered as constant (Figure 38d).

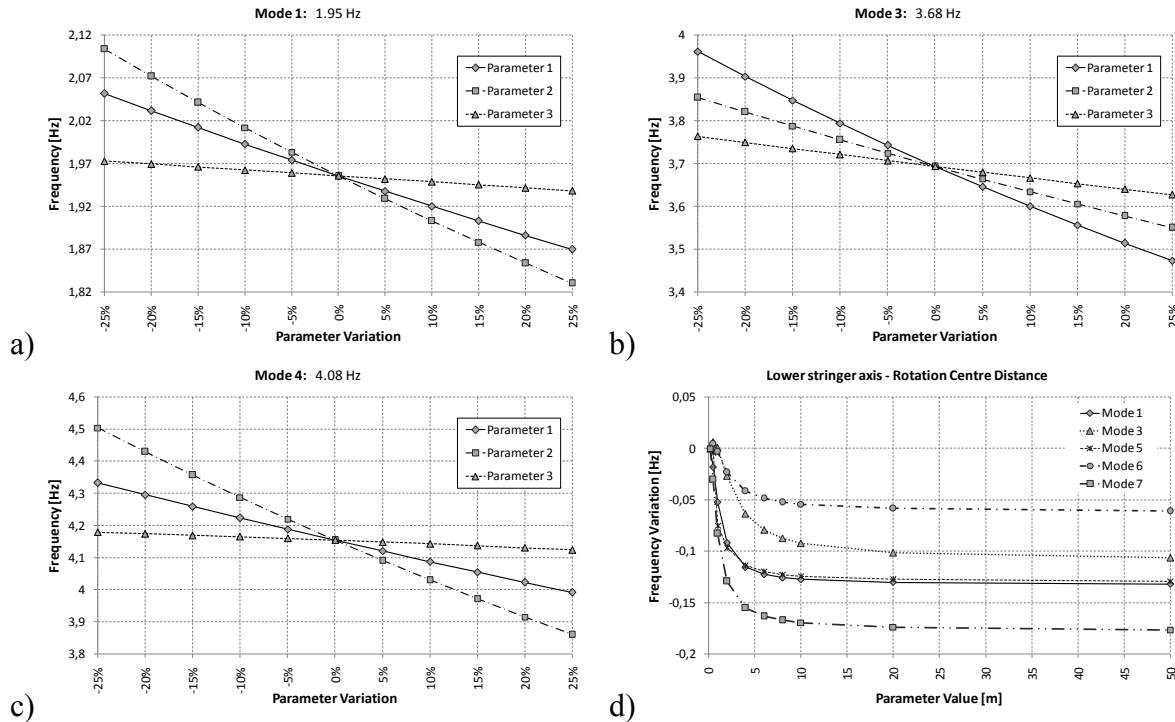


Figure 38: Sensitivity functions of parameter n° 1-2-3-5-6-7 calculated for vibration modes n° 1-3-4

The modeFRONTIER procedure converged to stable parameter configurations after 3560 cycle iterations, taking less than 15 seconds for each cycle for a total computation time equal to 15 hours. The numerical optimization permitted to obtain an updated model characterized by numerical eigenfrequencies very similar to the experimental results (maximum difference of about 4.5%) and high MAC values, reported in Table 6. The complete MAC matrix is reported in Figure 39.

Parameter n°	Initial Value	Final Value	Mode n°	Numerical Freq. [Hz]	Experimental Freq. [Hz]	$\Delta$ [%]	MAC
1	9027 kg/m <sup>3</sup>	7897 kg/m <sup>3</sup>	1	1.82	1.77	2.73	98.7%
2	17477 kg/m <sup>3</sup>	18735 kg/m <sup>3</sup>	2	3.64	3.65	0.33	98.3%
3	16854 kg/m <sup>3</sup>	18068 kg/m <sup>3</sup>	3	3.64	3.68	1.06	82.7%
4	0.17 m	76.00 m	4	4.13	4.08	1.27	72.7%
5	124860 kN*m	93645.00 kN*m	5	6.59	6.86	4.00	72.0%
6	230690 kN*m	183270 kN*m	6	10.66	10.93	2.52	75.9%
7	1068800 kN/m	1068800 kN/m	7	12.91	12.35	4.53	68.4%

Table 6: Updated FE Model: in initial/final values of parameters and numerical/experimental frequencies

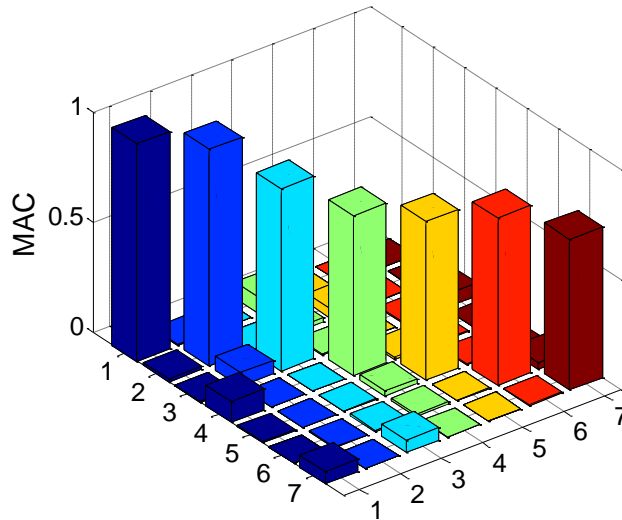


Figure 39: Graphical representation of numerical/experimental MAC matrix

## 6 ADVANCED FATIGUE ASSESSMENT

The Updated FE Hinge model of Panaro bridge was used for a further fatigue assessment of case study, comparing results obtained from an advanced modeling/updating approach with standard methodologies. Indeed, one main objective of Fadless Project is the critical review of standard approaches currently adopted for the fatigue assessment of complex structures like bridges. In particular, the Project aims also at evaluating the effectiveness of standard FE modeling techniques and fatigue load models, comparing theoretical results obtained from current design rules with experimental data. From this point of view, the comparison between fatigue damages calculated by an updated model and a standard one constitute a preliminary results in such critical review process.

The number (Figures 39 and 40) and distribution (Figure 41) of damaged components is similar to the standard results calculated by the Hinge Model, while damage intensities are a little lower. From the fatigue assessment point of view, the updating process didn't showed to vary significantly the results obtainable from a global FE model, thus confirming the necessity of refined local analysis of critical details in order to catch properly the actual stress spectra induced by distortion and vibration phenomena.

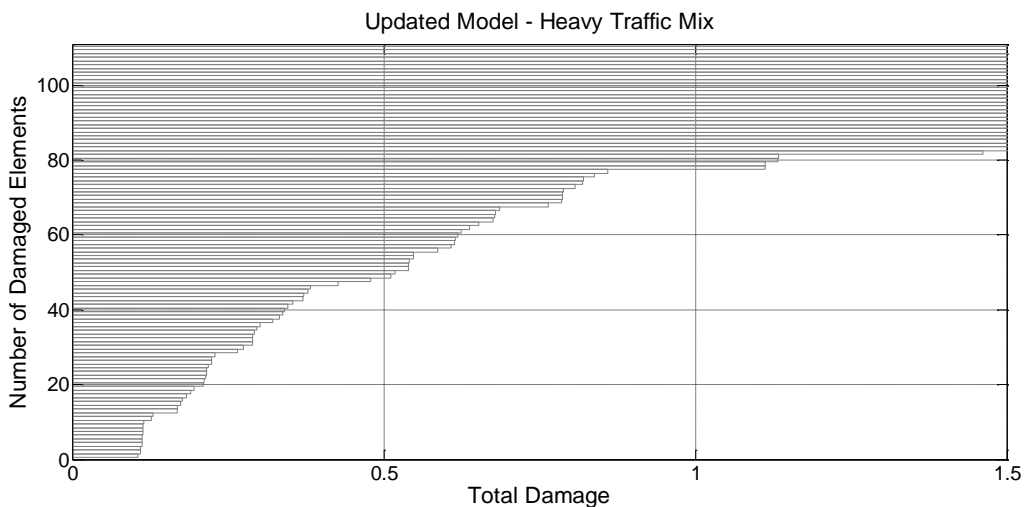


Figure 39: Updated Model - Standard Traffic Mix Damage

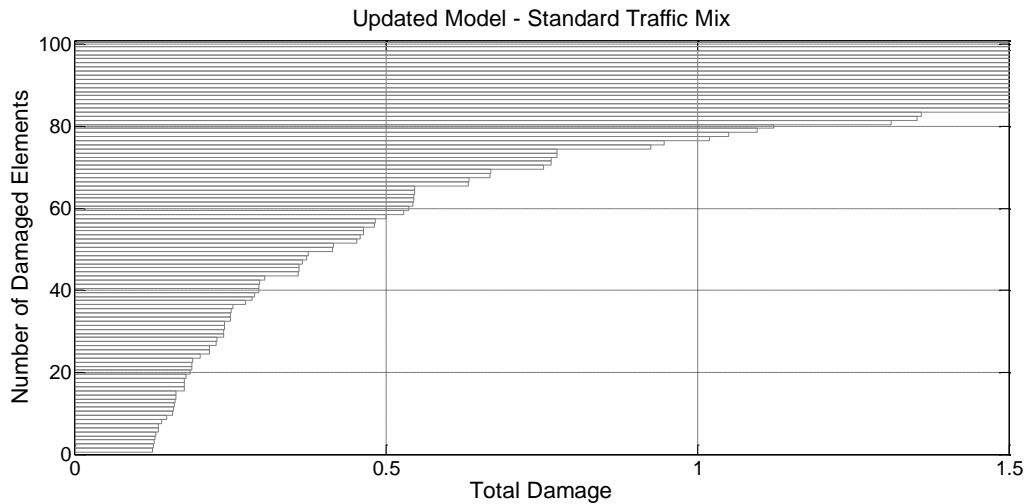


Figure 40: Updated Model - Standard Traffic Mix Damage

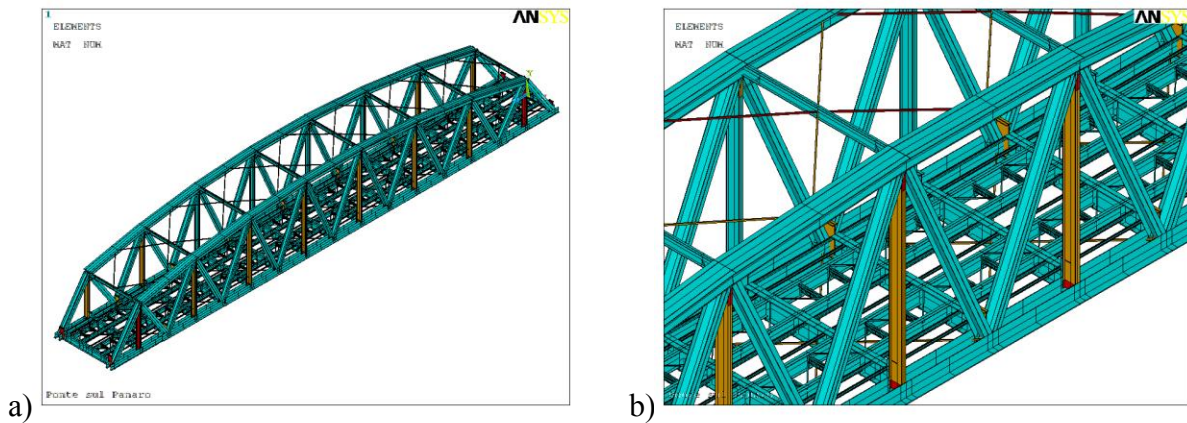


Figure 41: Updated FE Models - Heavy Traffic Mix: general (a) and detailed (b) graphical representation of damaged components (Yellow elements:  $-0.1 < \text{Damage} < 1$  --- Red elements:  $\text{Damage} > 1$ )

## 7 SOME PRELIMINARY REMARK

Main objective of FADLESS Project are the development of enhanced approaches for the correct evaluation of fatigue damages on steel railway bridges considering in particular the distortion and vibration effects.

The theoretical and experimental analysis performed on Italian case study, the Panaro bridge, permitted to obtain very interesting preliminary results concerning the actual dynamic behavior of such complex structures and the effectiveness of currently adopted modeling approaches at representing the internal distribution of forces/stresses. In particular, standard FE models were used for the fatigue assessment of the bridge, realized according to Eurocode rules. Experimental dynamic analysis permitted to identify global/local vibration modes and to constitute a suitable base for the subsequent numerical updating of developed FE model, obtained by an automatic optimization procedure. Advanced fatigue assessment was performed on the updated FE model and related results were compared to standard ones.

Moreover, critical details concerning the distortion/vibration induced fatigue damages were identified; such details, in the second part of the project, will be the object of further studies including the development of local FE models and the realization of sub-structuring analysis.

At last, suitable long-term monitoring systems will be designed and installed on all case studies in order to identify the actual railway traffic spectra on European bridges, providing the necessary base for a critical review of actually adopted fatigue load models.

## REFERENCES

- [1] EN 1993-1-9, 2002. Eurocode 3: Design of steel structures - Part 1.9: Fatigue strength of steel structures. CEN European Committee for Standardization.
- [2] AREMA, 2005. Manual of railway engineering. Washington D.C: American Railway Engineering and Maintenance of Way Association (AREMA).
- [3] Ferrovie dello Stato, 1992. Istruzione n. 44f del 30.01.1992: Verifiche a fatica dei ponti ferroviari metallici. Ente Ferrovie dello Stato (in Italian).
- [4] Ferrovie dello Stato, 1997. Istruzione n. I/SC/PS-OM/2298 del 2.6.1995 "Sovraccarichi per il calcolo dei ponti ferroviari - Istruzioni per la progettazione, l'esecuzione ed il collaudo". Ente Ferrovie dello Stato (in Italian).
- [5] European Commission, Energy and Transport DG, 2005. TEN-T Trans-European Transport Network: priority axes and projects 2005. Technical report, European Commission. (ec.europa.eu).
- [6] Goicolea, J., 2004. "Dynamic loads in new engineering codes for railway bridges in Europe and Spain". In Bridges for High-Speed Railways, June 3-4; Porto.
- [7] Kühn, B., Lukić, M., Nussbaumer, A., Günter, H.P., Helmerich, R., Herion, S., Kolstein, M.H., Walbridge, S., Androic, B., Dijkstra, O., Bucak., 2008. Assessment of Existing Steel Structures: Recommendations for Estimation of Remaining Fatigue Life. Report EUR 23252 EN - 2008, European Community.
- [8] Fisher, J.W., 1984. Fatigue and fracture in steel bridges: case studies. John Wiley.
- [9] Fisher, J.W. and Roy, S., 2008. "Fatigue of steel infrastructure". Proc. of Bridge Maintenance, Safety Management, Health Monitoring and Informatics IABMAS08 Conference, July 13 17 2008, Seoul. Korea.
- [10] ANSYS Inc. (2005). ANSYS User Manuals Version 10. ANSYS Inc. Global Headquarters, Canonsburg, PA.
- [11] UNI EN 1991-2, 2005. Eurocode 1: Actions on structures - Part 2: Traffic loads on bridges. CEN European Committee for Standardization.
- [12] Taras, A. and Greiner, R., 2009. Development and Application of a Fatigue Class Catalogue for Riveted Bridge Components. Report ECCS TC6 - 2009 - xxx, Institute for Steel Structures and Shell Structures - Graz University of Technology, Graz. Austria.
- [13] LMS International (2005). LMS TestLab Rev6A: Operational Modal Analysis User Manual
- [14] ESTECO srl (2007). modeFRONTIER User Manual Version 4.0b.